ISSN 1392 - 1207. MECHANIKA. 2010. Nr.4(84)

Meshless analysis of cracked functionally graded materials under thermal shock

M.B. Nazari*, M. Shariati, M.R. Eslami***, B. Hassani******

**Shahrood University of Technology, 36199, 95161 Shahrood, Iran, E-mail: mbnazari@yahoo.com*
***Shahrood University of Technology, 36199, 95161 Shahrood, Iran, E-mail: mshariati@shahroodut.ac.ir*
****Amirkabir University of Technology, 15914 Tehran, Iran, E-mail: eslami@aut.ac.ir*
*****Shahrood University of Technology, 36199, 95161 Shahrood, Iran, E-mail: b_hassani@shahroodut.ac.ir*

1. Introduction

Functionally graded materials (FGMs) are a new type of advanced composites that are introduced for use in high temperature environments. The composition, microstructure and/or crystal structure of the FGMs change gradually which lead to form a nonhomogeneous material with continuously varying thermomechanical properties. In recent years, FGMs have been used widely in other applications [1].

According to the experimental studies of Kawasaki and Watanabe [1], when sudden cooling is applied to ceramic/metal FGMs, some edge cracks are created on the ceramic surface. Therefore, examining the surface crack problem in FGMs under thermal loading, especially thermal shock, is important in failure analysis of these materials.

Jin and Noda [2] derived the general form of the thermoelastic crack-tip fields in FGMs. They assumed that the material properties are continuous and piecewise differentiable function of spatial position and some of them are not zero at the crack-tip. According to their study, the variation of material properties does not affect the order of singularity of thermoelastic crack-tip fields. Kishimoto et al. [3] showed that in the presence of thermal loading, the path independency of original *J*-integral is lost. They presented a path-independent form of *J*-integral included extra term to regard the thermal effect. Analytical approaches including perturbation method and singular integral equations have been used to consider thermal fracture of FGMs [4, 5]. It is important to know that using analytical approaches is limited to some simple problems or especial conditions. For example, Noda and Guo [5] have studied the edge crack problem in FGMs under thermal shock using the perturbation method. For the sake of simplification, they assumed that the Poisson's ratio is constant. Yildirim [6] and Dag [7] developed an equivalent domain integral to compute the mode-I stress intensity factor (SIF) under steady-state and transient thermal loading in isotropic and orthotropic FGMs, respectively. Dag and Yildirim [8] implemented the J_k-integral to evaluate the mixed-mode stress intensity factors in FGMs under thermal loading. These analyses were performed by using very fine meshes of regular elements in HEAT2D and FRAC2D software. KC and Kim [9] used the interaction integral to evaluate the mixed-mode SIFs under steady-state thermal loading. Chen [10] used interaction integral in conjunction with element-free Galerkin (EFG) method to compute SIFs for an interface crack in orthotropic functionally graded coating under steady-state thermal loading. These results were obtained by using first-order polynomial basis functions which lead to a fine node arrangement. Also, Chen reported the value of *J*-integral was not completely path-independent and results were unreliable for small integral domain sizes.

The EFG method provides an efficient and robust framework to analyze fracture mechanics problems. This method has been implemented for fracture analysis of cracks in FGMs under mechanical loading e.g. [11] or steady-state thermal stresses [10]. In this paper, the EFG method is applied in both steady-state and transient thermal fracture of FGMs. The transient thermal loading is imposed in the form of thermal shock.

This paper is organized as follows. Section 2 presents the thermoelastic governing equations. Section 3 provides the EFG discretization form of governing equations. Section 4 explains the use of the equivalent domain integral for thermal fracture of FGMs. Section 5 describes the modal decomposition technique to obtain the transient temperature field. Section 6 presents numerical results and discussion about the relevant aspects of the results. Finally, section 7 draws conclusions.

2. Governing equations

A body occupying a space Ω surrounded by a surface Γ under external and body forces and prescribed thermal boundary conditions has been considered. The governing equations for static linear thermoelasticity in the domain Ω are

$$\nabla.\boldsymbol{\sigma} + \boldsymbol{b} = 0 \tag{1}$$

$$-\nabla \boldsymbol{q} + Q = \rho c \frac{\partial T}{\partial t} \tag{2}$$

Also, the heat flux is obtained based on the Fourier law

$$\boldsymbol{q} = -k\boldsymbol{I}\nabla T \tag{3}$$

The constitutive equation is defined as

$$\boldsymbol{\sigma} = \tilde{\boldsymbol{C}}:\left(\boldsymbol{\varepsilon} - \boldsymbol{\varepsilon}^{th}\right) \tag{4}$$

where

$$\boldsymbol{\varepsilon} = \nabla_s \boldsymbol{u} \tag{5}$$

$$\boldsymbol{\varepsilon}^{th} = \alpha\left(T - T_0\right)\boldsymbol{I} \tag{6}$$

Here, the material properties are the forth-order Hooke tensor $\tilde{\boldsymbol{C}}$, isotropic conductivity k, expansion coefficient α, density ρ and specific heat c. The field variables are displacement $\boldsymbol{u}$, strain tensor $\boldsymbol{\varepsilon}$, stress tensor $\boldsymbol{\sigma}$, and thermal strain $\boldsymbol{\varepsilon}^{th}$ and the imposed values are heat source Q and body force $\boldsymbol{b}$. $\boldsymbol{I}$ is the identity second-order tensor and ∇_s is the symmetric gradient operator on a vector field. The boundary conditions are as follows

$$T = \overline{T} \quad \text{on } \Gamma_T \tag{7}$$

$$k\boldsymbol{I}\nabla T.\boldsymbol{n} = \overline{q} \quad \text{on } \Gamma_q \tag{8}$$

$$k\boldsymbol{I}\nabla T.\boldsymbol{n} + h\left(T - T_\infty\right) = \overline{q} \quad \text{on } \Gamma_c \tag{9}$$

$$\boldsymbol{u} = \overline{\boldsymbol{u}} \quad \text{on } \Gamma_u \tag{10}$$

$$\sigma.\boldsymbol{n} = \overline{\boldsymbol{t}} \quad \text{on } \Gamma_t \tag{11}$$

where h is the convection coefficient and $\boldsymbol{n}$ is the outward unit vector which is normal to Γ.

3. Element-free Galerkin method in thermoelasticity

We implement the EFG method to solve governing partial differential equations (PDEs) of 2D thermoelastic problems. This method needs only a set of nodes to construct the discretized model. In EFG, using moving least square (MLS) approximation leads to stability in function approximation and applying the Galerkin procedure provides stable and well-behaved system of discretized equations. Here we use the EFG discretization in the space dimensions only and follow the Kantorovitch semi-discretization process. According to the EFG method, the final discrete equations can be obtained as

$$\boldsymbol{C}^{th}\dot{\boldsymbol{T}} + \left(\boldsymbol{K}^{th} + \boldsymbol{K}_\gamma^{th}\right)\boldsymbol{T} = \boldsymbol{F}^{th} + \boldsymbol{F}_\gamma^{th} \tag{12}$$

$$\left(\boldsymbol{K} + \boldsymbol{K}^\gamma\right)\boldsymbol{U} = \boldsymbol{F} + \boldsymbol{F}^\gamma \tag{13}$$

where the dot (.) denotes differentiation with respect to time and

$$\boldsymbol{C}_{ij}^{th} = \int_\Omega \rho c \varphi_i \varphi_j d\Omega \tag{14}$$

$$\boldsymbol{K}_{ij}^{th} = \int_\Omega k\boldsymbol{B}_i^{thT}\boldsymbol{B}_j^{th} d\Omega + \int_{\Gamma_c} h\varphi_i\varphi_j d\Gamma \tag{15}$$

$$\boldsymbol{K}_{ij}^{\gamma} = \gamma\int_{\Gamma_u} \boldsymbol{\varphi}_i^T\boldsymbol{S}\boldsymbol{\varphi}_j d\Gamma \tag{16}$$

$$\boldsymbol{F}_i^{th} = \int_\Omega Q\varphi_i d\Omega + \int_{\Gamma_q} \overline{q}\,\varphi_i d\Gamma + \int_{\Gamma_c} hT_\infty\varphi_i d\Gamma \tag{17}$$

$$\boldsymbol{F}_i^{\gamma} = \gamma\int_{\Gamma_u} \boldsymbol{S}\overline{\boldsymbol{u}}\boldsymbol{\varphi}_i d\Gamma \tag{18}$$

where

$$\boldsymbol{B}_i^{th} = \begin{bmatrix} \partial\varphi_i/\partial x_1 \\ \partial\varphi_i/\partial x_2 \end{bmatrix} \tag{19}$$

and

$$\boldsymbol{K}_{ij} = \int_\Omega \boldsymbol{D}\boldsymbol{B}_i^T\boldsymbol{B}_j d\Omega \tag{20}$$

$$\boldsymbol{K}_{ij}^{\gamma} = \gamma\int_{\Gamma_u} \boldsymbol{\varphi}_i^T\boldsymbol{S}\boldsymbol{\varphi}_j d\Gamma \tag{21}$$

$$\boldsymbol{F}_i = \int_\Omega \boldsymbol{b}\boldsymbol{\varphi}_i^T d\Omega + \int_{\Gamma_t} \bar{\boldsymbol{t}}\boldsymbol{\varphi}_i^T d\Gamma \tag{22}$$

$$\boldsymbol{F}_i^{\gamma} = \gamma\int_{\Gamma_u} \boldsymbol{S}\overline{\boldsymbol{u}}\boldsymbol{\varphi}_i d\Gamma \tag{23}$$

where

$$\boldsymbol{S} = \begin{bmatrix} S_1 & 0 \\ 0 & S_2 \end{bmatrix}, S_i = \begin{cases} 1 & \text{if } u_i \text{ given on } \Gamma_u \\ 0 & \text{if } u_i \text{ not given on } \Gamma_u \end{cases} \tag{24}$$

$$\boldsymbol{B}_i = \begin{bmatrix} \partial\varphi_i/\partial x_1 & 0 \\ 0 & \partial\varphi_i/\partial x_2 \\ \partial\varphi_i/\partial x_2 & \partial\varphi_i/\partial x_1 \end{bmatrix} \tag{25}$$

$$\boldsymbol{\varphi}_i = \begin{bmatrix} \varphi_i & 0 \\ 0 & \varphi_i \end{bmatrix} \tag{26}$$

In the enriched EFG method, the singularity problems due to the presence of a crack are alleviated by enrichment functions. In the intrinsic enrichment, the standard basis (usually polynomials) vector is enriched by including the near-tip asymptotic displacement field as [12]

$$\boldsymbol{p}^T(\boldsymbol{x}) = \left\{ \begin{matrix} 1, x_1, x_2, \sqrt{r}cos\frac{\theta}{2}, \sqrt{r}sin\frac{\theta}{2}, \\ \sqrt{r}sin\frac{\theta}{2}sin\theta, \sqrt{r}cos\frac{\theta}{2}sin\theta \end{matrix} \right\} \tag{27}$$

where r and θ are the usual crack-tip polar coordinates.

4. Equivalent domain integral for thermal fracture

The J-integral is an energy-based method which is widely used to calculate SIFs e.g., [13]. The J-integral originally was derived in the form of contour integral [14]

$$J = \int_{\Gamma_A} (W\delta_{1j} - \sigma_{ij}u_{i,1})n_j\, d\Gamma_A \tag{28}$$

where Γ_A is an arbitrary contour enclosing the crack-tip and n_j is the jth component of the outward unit vector normal to Γ_A. Because of calculating purpose, it is suitable this contour form is converted into an equivalent domain integral (EDI). Defining a smooth weight function q and applying divergence theorem, the equivalent domain form of J-integral is derived as [6]

$$J = \int_A (\sigma_{ij}u_{i,1} - W\delta_{1j})q_{,j} dA + \int_A (W_{,1})_{expl} q dA \tag{29}$$

where A is the area inside the contour Γ_A. The second integral contains $(W_{,1})_{expl}$ i.e., the explicit partial derivatives of W with respect to x_1. It should be noted that in FGMs temperature field and material properties are dependent on the spatial coordinates. In linear elastic fracture mechanics, J-integral is equal to the energy release rate and the relationship between the energy release rate and the mode-I SIF is given by

$$J = K_I^2 / E_{tip}^* \tag{30}$$

where $E^*_{tip} = E_{tip}$ for plane stress and $E_{tip}/(1-\nu^2_{tip})$ for plane strain. E_{tip} and ν_{tip} are Young's modulus and Poisson's ratio, respectively, evaluated at the crack-tip.

5. Transient heat conduction problem

To obtain temperature field, we should solve the first-order matrix differential Eq. (12). Among many methods, we choose the modal decomposition technique [15]. Modal decomposition is an analytical approach to solve systems of ordinary differential equations (ODEs) without the introduction of additional approximations. Based on modal decomposition procedure, a coupled system of ODEs is turned into uncoupled equations by using eigenvectors. The solution of Eq. (12) can be expressed as linear combination of all eigenvectors of the homogenous system $\boldsymbol{T}(t) = [\boldsymbol{T}_1 \quad \boldsymbol{T}_2 \quad \cdots \quad \boldsymbol{T}_N]\boldsymbol{\psi}(t) = \boldsymbol{M}\boldsymbol{\psi}(t)$, where $\boldsymbol{M}$ is an $N \times N$ square matrix whose columns are the eigenvectors. Substituting above definition into Eq. (12) and premultiplying it by $\boldsymbol{M}^T$, we can obtain the uncoupled system of equation

$$\boldsymbol{C}^{th*}\dot{\boldsymbol{\psi}} + \boldsymbol{K}^{th*}\boldsymbol{\psi} = \boldsymbol{M}^T\left(\boldsymbol{F}^{th} + \boldsymbol{F}^{th}_{\gamma}\right) \tag{31}$$

where

$$\boldsymbol{K}^{th*} = \boldsymbol{M}^T\boldsymbol{K}^{th}\boldsymbol{M}\,,\ \boldsymbol{C}^{th*} = \boldsymbol{M}^T\boldsymbol{C}^{th}\boldsymbol{M} \tag{32}$$

The system of Eq. (31) contains N uncoupled equations

$$\dot{\psi}_i + s_i\psi_i = \frac{\Lambda_i}{\boldsymbol{C}^*_{ii}} \quad (i=1, 2,\ldots, N) \tag{33}$$

where $s_i = \boldsymbol{K}^{th*}_{ii} / \boldsymbol{C}^{th*}_{ii}$ and $\boldsymbol{\Lambda}=\boldsymbol{M}^T(\boldsymbol{F}^{th}+ \boldsymbol{F}^{th}_{\gamma})$. The initial condition $\boldsymbol{\psi}(0)$ can be obtained from $\boldsymbol{T}(0) =\boldsymbol{M}\,\boldsymbol{\psi}(0)$. Depending on the complexity of right-hand side of Eq. (31), it is solved either analytically or numerically.

6. Numerical results and discussion

In this section, we consider calculation of the mode I stress intensity factor for an edge crack in functionally graded plate (FGP) under thermal stresses. The distribution of material properties is determined by means of continuum functions, e.g., exponential function or micromechanics models, e.g., self-consistent model. The following examples are presented:

1. an edge cracked plate: exponentially gradation;
2. an edge cracked plate: linear gradation;
3. composite strip with an edge crack;
4. edge crack in an FGP: micromechanics model.

The FGP of length W and height H with a crack of length a is considered. The thickness (in the x_3 direction) of plate is assumed quite thin for plane stress analysis and large enough for plane strain analysis. The crack is aligned parallel to the direction of material property gradation. Initially, the FGP is at a uniform stress-free temperature T_0. The thermal boundary conditions are applied on the $x_1 = 0$ and $x_1 = W$ faces. All other faces, including the crack surfaces, are assumed to be insulated which results in a one dimensional heat conduction problem in the x_1 direction. In all cases, the calculated SIFs will be normalized by dividing to

$$K_0 = E(0)\alpha(0)T_0\sqrt{\pi a}/(1-\nu(0))\,. \tag{34}$$

6.1. An edge cracked plate: exponentially gradation

An unconstrained FGP with an edge crack of length a as shown in Fig. 1, a is considered. Fig. 1, b presents the complete node arrangement of the FGP which consists of 1695 regular nodes and 40 crack-tip nodes, with a total of 1735. Fig. 1, c shows the crack-tip node arrangement. In this case, the FGMs with exponentially varying thermomechanical properties, in the x_1 direction, (for E, ν, α, k, ρc) are considered, e.g., as

$$E(x_1) = E(0)\,exp(P_E x_1) \tag{35}$$

where the nonhomogeniety parameters are define, e.g., as

$$P_E = \frac{1}{W}ln\left(\frac{E(W)}{E(0)}\right) \tag{36}$$

Here, the ceramic/metal ZrO_2/Ti-6Al-4V material with properties of Table 1 is assumed.

For the sake of comparison, two different cases of the thermal boundary conditions are considered in the steady-state analysis. In the third case, a transient analysis is also carried out for different temperatures at the left and right sides of the plate.

In order to verify the implementation of the displacement correlation technique (DCT) which is a convenient direct method for evaluation of SIF [16] and EDI approach in the framework of EFG method, we first present comparisons of the calculated SIFs and the available reference solutions. In this case, the temperature of $x_1 = 0$ and $x_1 = W$ faces are decreased from T_0 to T_1 and T_2, respectively.

Table 1

Material properties of ZrO_2 and Ti-6Al-4V

Materials	Young's modulus, GPa	Poisson's ratio	Coefficient of thermal expansion 10^{-6} /K	Thermal conductivity, W/(m K)	Mass density, kg/m^3	Specific heat, J/(kg K)
ZrO_2	151.0	0.33	10.0	2.09	5331	456.7
Ti-6Al-4V	116.7	0.33	9.5	7.5	4420	537.0

Table 2 compares the normalized SIFs with the results provided by Erdogan and Wu [4], KC and Kim [9] and Yildirim [6]. As shown in Table 2, the obtained solutions are in good agreement with the references. It is interesting to note that our model is comprised of 1735 nodes, while the 2D mesh discretization in KC and Kim [9] consists of 966 elements and 2937 nodes in the framework of the finite element method.

Table 2

Normalized mode I SIF in FGP under steady-state thermal loading

Material parameters	Load	Analysis type	Normalized SIF				
			Present		Erdogan and Wu [4]	KC and Kim [9]	Yildirim [6]
			EDI	DCT			
WP_E=ln(5) WP_α=ln(2)	T_1=0.5T_0	Plane strain	0.0124	0.0126	0.0125	0.0128	0.0128
	T_2=0.5T_0	Plane stress	0.0090	0.0088	–	0.0090	0.0090
	T_1=0.05T_0 T_2=0.05T_0	Plane strain	0.0246	0.0240	0.0245	0.244	–
WP_E=ln(5) WP_α=ln(2) WP_k =ln(10)	T_1=0.2T_0	Plane strain	0.0334	0.0343	0.0335	0.0334	0.034
	T_2=0.5T_0	Plane stress	0.0234	0.0239	–	0.0235	0.024
	T_1=0.05T_0 T_2=0.5T_0	Plane strain	0.0405	0.0411	0.0410	0.0406	–

Since the surface crack is usually created during cooling, the FGP problem subjected to a cooling shock is here considered. To consider the thermal shock, we assume that the FGP is initially at a uniform stress-free temperature T_0 and suddenly cooled down to constant temperatures T_1 and T_2 at the left and right hand side faces, respectively. The assumed values are T_1=0.25 T_0 and T_2=0.75 T_0.

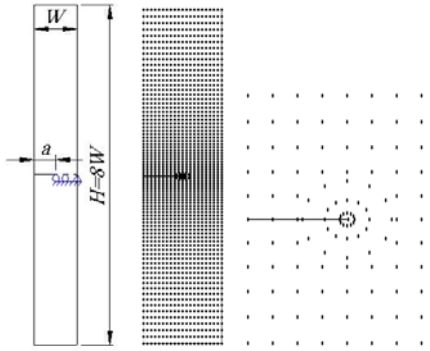

Fig. 1 An FGM plate with an edge crack: a - geometry, b - complete node arrangement, c - crack-tip node arrangement

The obtained results for the transient temperature distribution in the ZrO_2/Ti-6Al-4V FGM versus normalized time τ, as is defined in Eq. (37), is depicted in Fig. 2.

$$\tau = \frac{k(0)/\rho(0)c(0)}{W^2}t \tag{37}$$

According to these results, the temperature gradient near the plate edges is considerably large at the early times after imposing the thermal shock. This large temperature gradient leads to significantly large tensile stresses near the edges of FGP [4]. Here, we assume that ΔT = = $T(x_1,t)$ - T_0. Also, these transient temperature and others in the next examples indicate that the modal decomposition technique is an efficient tool to obtain the transient temperature distribution in thermal shock problems. Because the order of time points in which analysis is performed varies between -4 and 2.

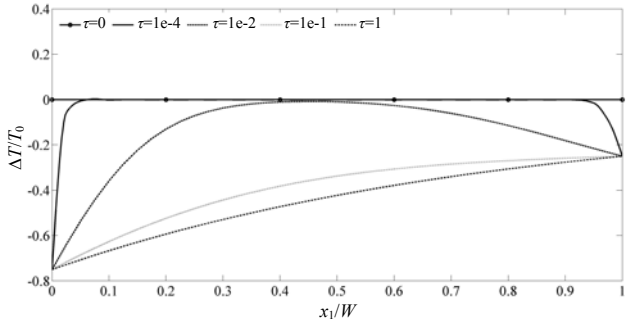

Fig. 2 Transient temperature distribution in the FGP (ZrO_2/Ti-6Al-4V) for various normalized time with T_1/T_0 = 0.25 and T_2/T_0 = 0.75

Figs. 3 and 4 present normalized SIFs in the ZrO_2/Ti-6Al-4V plate resulting from the transient temperature field versus the normalized time τ and the normalized crack length a/W for plane strain and plane stress cases, respectively. As shown in these figures, the SIF increases quickly to a peak value that is drastically larger than steady value and then decreases rapidly to the corresponding steady value for all crack lengths. In addition, the magnitude of SIF decreases as the normalized crack length a/W becomes larger in both transient and steady states that are in agreement with the results recently reported by Noda and Guo [5]. As the final point, the magnitude of SIF for plane strain is larger than plane stress. Noda et al. [17] have derived thermal stresses analytically for a homogeneous isotropic strip under one-dimensional transient temperature distribution. These results indicate that the thermal stresses for the plane strain case are equal to those of plane stress multiplied by a factor of 1/(1 - ν). Regarding the fact $0 < \nu < 0.5$, this factor is greater than one, that implies a larger SIF for the plane strain in comparison with

the plane stress problem, which can be noticed from Figs. 2 and 3. The agreement between SIFs evaluated by means of EDI and DCT is found to be acceptable.

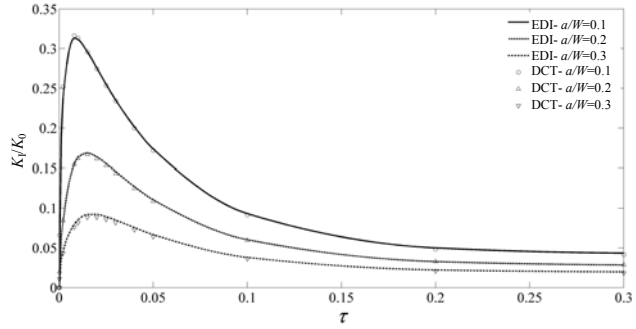

Fig. 3 Normalized mode I SIF in the ZrO_2/Ti-6Al-4V plate versus normalized time and different crack lengths in plane strain condition

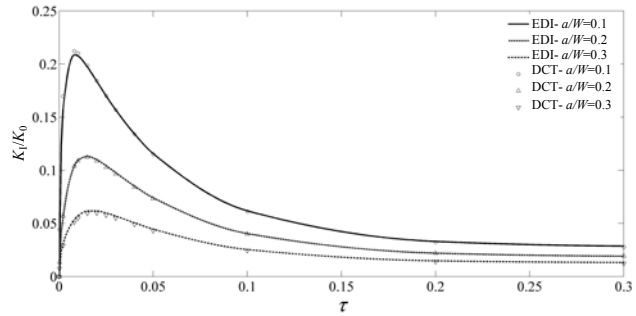

Fig. 4 Normalized mode I SIF in the ZrO_2/Ti-6Al-4V plate versus normalized time for different crack lengths in plane stress condition

6.2. An edge cracked plate – linear gradation

The configuration of the first example is considered here assuming a linear gradation for material properties. Moreover, a different set of thermal boundary conditions is imposed on the uncracked face of FGP. To apply a thermal shock, the cracked face is assumed to be quenched to a constant temperature of $T_1 = 0.15\ T_0$ while having the free convection at other face with a convection coefficient of $h = 1$ W/(m^{2}K) and the ambient temperature is assumed T_0. The transient temperature distribution in the ZrO_2/Ti-6Al-4V plate is presented in Fig. 5. The effect of the convection at the x_1=W face on the temperature distribution is observed at the steady-state. Figs. 6 and 7 show the transient thermal SIF versus crack lengths for plane strain and plane stress cases, respectively. As it is seen, the variation of the thermal SIF is the same as the previous example. The effect of the thermal boundary condition applied on the uncracked face, is illustrated in the Fig. 8. Here, the $h = 0$ corresponds to the insulated thermal boundary condition and $h = \infty$ corresponds to the known temperature boundary condition. According to this figure, while the value of the SIF is independent of the type of the thermal boundary condition applied on the uncracked face, the steady-state value is completely dependent on. Moreover, a greater value for the steady-state SIF is obtained for the case of constant temperature faces.

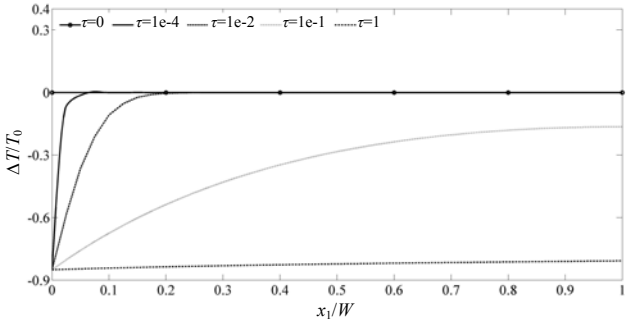

Fig. 5 Transient temperature distribution in the ZrO_2/Ti-6Al-4V plate for various normalized times with $T_1/T_0 = 0.15$ and free convection at $x_1 = W$

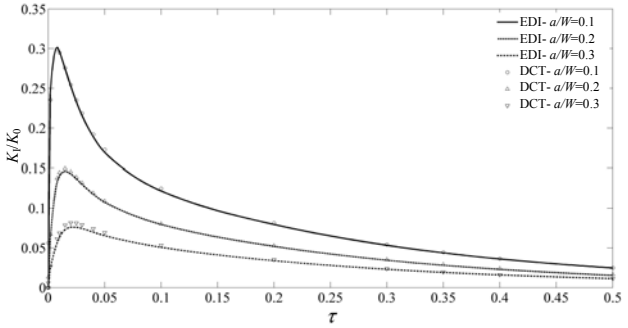

Fig. 6 Normalized mode I SIF in the ZrO_2/Ti-6Al-4V plate versus normalized time and different crack lengths in plane strain condition

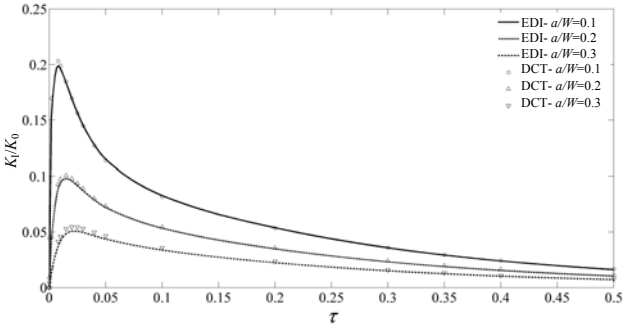

Fig. 7 Normalized mode I SIF in the ZrO_2/Ti-6Al-4V plate versus normalized time for different crack lengths in plane stress condition

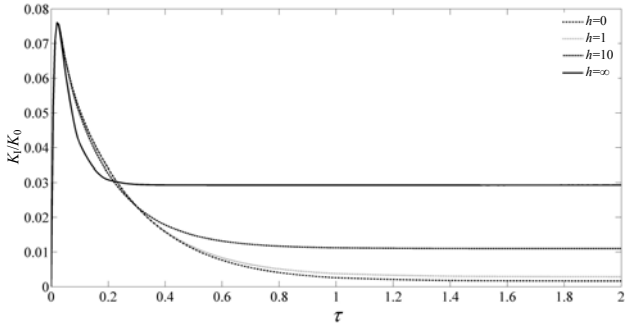

Fig. 8 The effect of thermal boundary condition at $x_1 = W$ on the variation of normalized thermal SIF

6.3. Composite strip with an edge crack

Crack analysis in composite structures requires consideration of the piecewise continuous nature of the material properties comprising the structure. Here, we consider a composite plate composed of two different materi-

als with an graded interface zone. The variation of material properties is approximated by a hyperbolic-tangent function as follows

$$E(x_1) = \frac{E(W)+E(0)}{2} + \frac{E(0)-E(W)}{2} \times \\ \times tanh(\eta_E(x_1+d)) \quad (38)$$

when $\eta \to \infty$ a jump occurs in the gradation of material properties across the interface at $x_1 = -d$. The configuration under consideration and the variation of the Young's modulus are shown in Figs. 9, a and b, respectively.

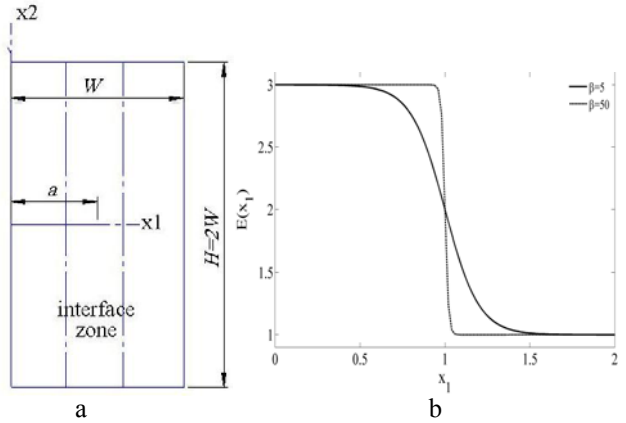

a b

Fig. 9 A cracked FGM plate (a) configuration (b) the variation of the Young's modulus in the FGP

The following data were used for the plane strain and plane stress cases

$a/W = 0.1 - 0.3$, $H/W = 2$

$d = -0.5$, $\eta_E = 15$, $\eta_v = \eta_\alpha = \eta_k = \eta_{\rho c} = 5$

$(E(W), E(0)) = (1,3)$, $(v(W), v(0)) = (0.1,0.3)$

$(\alpha(W), \alpha(0)) = (0.03,0.01)$

$(k(W), k(0)) = (3,1)$, $(\rho c(W), \rho c(0)) = (1,1)$

Here, we assume that only the left hand side face of the FGP is suddenly cooled down to the constant temperature $T_1 = 0$. The transient temperature distribution in the FGP versus normalized time τ, as is defined in Eq. (37), is depicted in Fig. 10. The effect of the conductivity difference of plate sides on the temperature distribution is clearly observed in the steady-state graph.

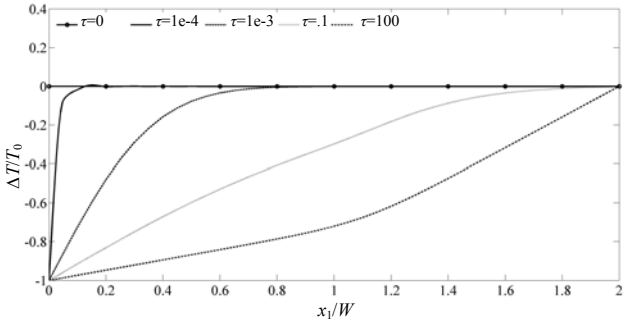

Fig. 10 Transient temperature distribution in the FGP for various normalized times with $T_1 = 0$ and $T_2/T_0 = 1$

Figs. 11 and 12 show transient thermal SIFs in the FGP versus the normalized crack length a/W for plane strain and plane stress cases, respectively. According to these figures, the SIF increases quickly to a peak value and then decreases rapidly until the crack is closed. The corresponding time of the crack closure increases as the crack length is increased. In this example, the crack closure was occurred in steady-state for all crack lengths.

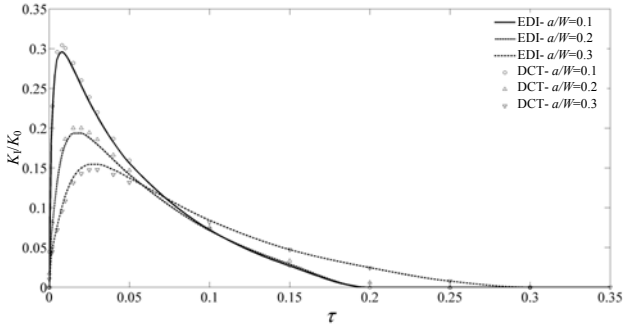

Fig. 11 Normalized mode I SIF in the FGP versus normalized time and crack length in plane strain condition

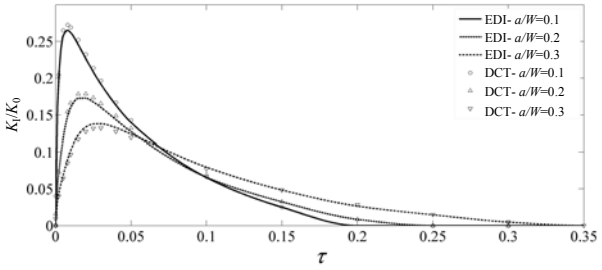

Fig. 12 Normalized mode I SIF in the FGP versus normalized time and different crack lengths in plane stress condition

6.4. Edge crack in an FGP: micromechanics model

Prediction of the effective macroscopic properties is one of the important problems of interest in composite material theory. For FGMs, as one of the graded composites, a few micromechanical models of composites have been developed. Among the micromechanical models developed for FGMs, the *self-consistent method* (SCM) is here used. Zuiker has been pointed out that the SCM provides a simple and initial estimate for the effective properties which is beneficial for the related optimal property distributions [18]. Moreover, in this method the properties are determined independent of the phases of inclusions and matrices. This is important for FGMs in which the volume fraction of the constituent phases varies in a wide range. For two-phase FGMs, the volume fraction of the ceramic and the metal phases are assumed in the form of a power function, i.e.,

$$V_c = 1 - (x_1/W)^p \quad (39)$$

$$V_m = 1 - V_c \quad (40)$$

in which W is the material gradation length and the exponent p is the gradient index. Here $x_1 = 0$ corresponds to the pure ceramic phase and $x_1 = W$ to the pure metal material. For two-phase composite, the effective material properties are determined from [18, 19].

$$\frac{1}{\kappa+4\mu/3}=\frac{V_c}{\kappa_c+4\mu/3}+\frac{V_m}{\kappa_m+4\mu/3} \tag{41}$$

$$\left(\frac{V_c\kappa_c}{\kappa_c+4\mu/3}+\frac{V_m\kappa_m}{\kappa_m+4\mu/3}\right)+$$
$$+5\left(\frac{V_c\mu_m}{\mu-\mu_m}+\frac{V_m\mu_c}{\mu-\mu_c}\right)+2=0 \tag{42}$$

$$\alpha=\alpha_m+\frac{(\alpha_c-\alpha_m)(1/\kappa-1/\kappa_m)}{(1/\kappa_c-1/\kappa_m)} \tag{43}$$

$$c=c_cV_c+c_mV_m\,,\ \rho=\rho_cV_c+\rho_mV_m \tag{44}$$

where the subscripts m and c stand for metal and ceramic phases, respectively. We consider an edge crack in an unconstrained FGP of length $W = 1$ and height $H = 8W$. With the purpose of imposing the thermal shock, we assume that only the cracked face of the FGP is suddenly cooled down to the constant temperature $T_1 = 0$ from the stress-free temperature T_0. The transient temperature distribution in the FGP is shown in Fig. 13.

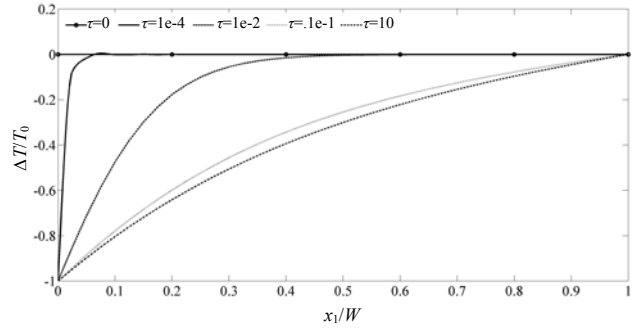

Fig. 13 Transient temperature distribution in the FGP for various normalized times with $T_1 = 0$ and $T_2/\ T_0 = 1$

Fig. 14 depicts the transient thermal SIF versus normalized crack lengths a/W for the plane strain case. Although the steady value of SIF is greater for longer cracks, the peak value of SIF is significantly larger for the short ones.

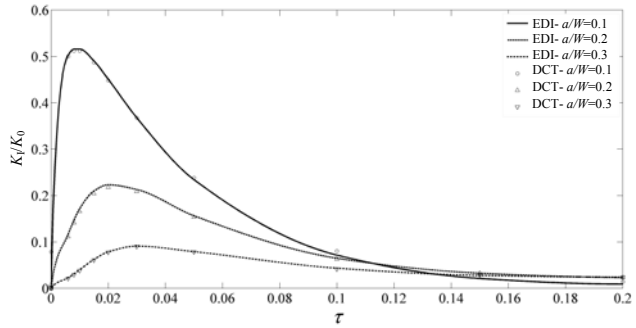

Fig. 14 Normalized mode I SIF in the FGP versus normalized time and different crack lengths in plane strain condition

7. Conclusions

In this paper, fracture behaviour of functionally graded materials under steady-state and transient temperature field is studied. Both domain form of J-integral (EDI) and displacement correlation technique (DCT) in conjunction with element-free Galerkin method are implemented to evaluate mode I stress intensity factor. The modal decomposition approach is used to obtain the transient temperature field analytically. The present study points out that:

1. In the enriched EFG framework a coarse mesh is sufficient to accurate analysis of cracks in FGMs under thermal loading.

2. At early time of thermal shock, the SIF gets to a large peak value which is significantly greater than corresponding steady value and then decreases rapidly to the steady value. Moreover, although the crack is closed at steady state for some cases, the value of SIF might be reach to a large positive peak value during the thermal shock period. These phenomenons imply that in thermal fracture analysis of FGMs, the SIF at the beginning of thermal loading might be the main factor in fracture failure analysis.

3. Comparison of numerical results with the reference solutions points out both energy-based EDI method and direct approach DCT in the framework of enriched EFG are efficient tools to analyze thermal fracture of FGMs.

References

1. **Kawasaki, A., Watanabe, R.** Thermal fracture behavior of metal/ceramic functionally graded materials. -Eng. Fracture Mechanics, 2002, v.69, p.1713-1728.
2. **Jin, Z-H., Noda, N.** Crack-tip singular fields in nonhomogeneous materials. -J. of Applied Mechanics, Trans. ASME, 1994, v.61, p.738-740.
3. **Kishimoto, K., Aoki, S., Sakata, M.** On the path independent J-integral. -Eng. Fracture Mechanics, 1980, v.13, p.841-850.
4. **Erdogan, F., Wu, B.H.** Crack problems in FGM layers under thermal stresses. -J. of Thermal Stresses, 1996, v.19, p.237-265.
5. **Noda, N., Guo, L.C.** Thermal shock analysis for a functionally graded plate with a surface crack. -Acta Mechanica, 2008, v.195, p.157-166.
6. **Yildirim, B.** An equivalent domain integral method for fracture analysis of functionally graded materials under thermal stresses. -J. of Thermal Stresses, 2006, v.29, p.371-397.
7. **Dag, S.** Thermal fracture analysis of orthotropic functionally graded materials using an equivalent domain integral approach. -Eng. Fracture Mechanics. 2006, v.73, p.2802-2828.
8. **Dag, S., Yildirim, B.** Computation of thermal fracture parameters for inclined cracks in functionally graded materials using Jk-integral. -J. of Thermal Stresses, 2009, v.32, p.530-556.
9. **KC, A., Kim, J.H.** Interaction integrals for thermal fracture of functionally graded materials.-Eng. Fracture Mechanics, 2008, v.75, p.2542-2565.
10. **Chen, J.** Determination of thermal stress intensity factors for an interface crack in a graded orthotropic coating-substrate structure. -Int. J. of Fracture, 2005, v.133, p.303-328.
11. **Nazari, M.B., Shariati, M.** Computation of stress intensity factor in functionally graded plates using element-free galerkin method. -Proceeding of 17th Int. Conference on Mech. Eng. ISME2009, 19-21 May, 2009, Tehran, Iran, p.279-280.

12. **Fleming, M., Chu, Y.A., Moran, B., Belytschko, T.** Enriched element-free galerkin methods for crack tip fields. -Int. J. for Numerical Methods in Eng., 1997, v.40, p.1483-1504.
13. **Stupak, E.** Investigation of fracture of inhomogeneous cast iron specimens. -Mechanika. -Kaunas: Technologija, 2010, p.20-24.
14. **Rice, J.R.** A path independent integral and the approximate analysis of strain concentration by notches and cracks. -J. of Applied Mechanics, 1968; 35:379.
15. **Zienkiewics, O.C., Taylor, R.L.** The Finite Element Method. -Oxford: Butterworth-Heinemann, 2000. -484p.
16. **Jakušovas, A., Daunys, M.** Investigation of low cycle fatigue crack opening by finite element method. -Mechanika. -Kaunas: Technologija, 2009, p.13-17.
17. **Noda, N., Hetnarski, R.B., Tanigawa, Y.** Thermal Stresses. -New York: Taylor and Francis, 2003.
18. **Zuiker, J.R.** Functionally graded materials: choice of micromechanics model and limitations in property variation. Composites Eng., 1995, v.5, p.807-819.
19. **Hill, R.** A self-consistent mechanics of composite materials. -J. of The Mechanics and Physics of Solids 1965, v.13, p.213-222.

M.B. Nazari, M. Shariati, M.R. Eslami, B. Hassani

FUNKCIONALIAI KOKYBIŠKŲ TERMIŠKAI APKRAUTŲ MEDŽIAGŲ SUIRIMO ANALIZĖ

R e z i u m ė

Analitiniu Galiorkino metodu atliekama kokybiškų medžiagų suirimo, esant I tipo nestacionariam terminiam apkrovimui, analizė. Įtempių intensyvumo koeficientai buvo nustatyti naudojant ekvivalentinį erdvinį integralą ir poslinkio koreliacijos metodą. Medžiagos mechaninėms savybėms apibūdinti buvo panaudotos kontinuumo funkcijos ir mikromechaninis modelis. Šiluminio šoko analizei taikytas modalinis suskaidymo metodas, kuris yra pusiau diskretinė priemonė nestacionariam temperatūros laukui nustatyti. Skaitinio tyrimo rezultatams patikrinti buvo pasinaudota kitų autorių darbais. Tyrimas parodė, kad įtempių intensyvumo koeficientas yra didžiausias pradinėje terminio šoko stadijoje, taigi ši stadija yra svarbi suirimo procesui.

M.B. Nazari, M. Shariati, M.R. Eslami, B. Hassani

MESHLESS ANALYSIS OF CRACKED FUNCTIONALLY GRADED MATERIALS UNDER THERMAL LOADING

S u m m a r y

The element-free Galerkin method which is enriched intrinsically is applied for fracture analysis of functionally graded materials under mode I steady-state and transient thermal loading. The stress intensity factors are evaluated by means of both equivalent domain integral and displacement correlation technique. Continuum functions and micromechanical model are used to describe the distribution of material properties. For thermal shock analysis, the modal decomposition method which is a semi-discretization approach is implemented to obtain the transient temperature field. The accuracy of numerical results is verified using the available reference solution. The results imply that the magnitude of the stress intensity factor gets to a large peak at the early time of the thermal shock which indicates its significant role in the fracture failure.

М.Б. Назари, М. Шариати, М.Р. Еслами, Б. Хассани

АНАЛИЗ РАЗРУШЕНИЯ ФУНКЦИОНАЛЬНО КАЧЕСТВЕННЫХ ТЕРМИЧЕСКИ НАГРУЖЕННЫХ МАТЕРИАЛОВ

Р е з ю м е

Аналитический метод Галеркина использован для анализа разрушения качественных материалов с применением I типа нестационарного термического нагружения. Коэффициент интенсивности напряжений определен при помощи эквивалентного пространственного интеграла и метода корреляции перемещения. Функции континуума и микромеханическая модель использована для описания механических характеристик материала. Для анализа теплового удара использован модальный метод разделения, который является полудискретным способом для определения постоянного температурного поля. Надежность полученных результатов оценена при помощи работ других авторов. Результаты исследования показали, что коэффициент интенсивности напряжении максимальное значение принимает в начальной стадии теплового удара, что подтверждает важность этой стадии для процесса разрушения.

Received June 18, 2010
Accepted August 27, 2010

DOI: 10.5755/j02.mech.15919